MAJOR ARTICLE

Staphylococcus aureus α-Hemolysin Mediates Virulence in a Murine Model of Severe Pneumonia Through Activation of the NLRP3 Inflammasome

Chahnaz Kebaier,[1] Robin R. Chamberland,[1,a] Irving C. Allen,[2] Xi Gao,[1] Peter M. Broglie,[1] Joshua D. Hall,[3] Corey Jania,[4] Claire M. Doerschuk,[2,4] Stephen L. Tilley,[4] and Joseph A. Duncan[1,2,5]

[1]Department of Medicine, Division of Infectious Diseases, [2]Lineberger Comprehensive Cancer Center, [3]Department of Microbiology and Immunology, [4]Department of Medicine, Division of Pulmonary and Critical Care Medicine, and [5]Department of Pharmacology, University of North Carolina, Chapel Hill

Staphylococcus aureus **is a dangerous pathogen that can cause necrotizing infections characterized by massive inflammatory responses and tissue destruction. Staphylococcal α-hemolysin is an essential virulence factor in severe *S. aureus* pneumonia. It activates the nucleotide-binding domain and leucine-rich repeat containing gene family, pyrin domain containing 3 (NLRP3) inflammasome to induce production of interleukin-1β and programmed necrotic cell death. We sought to determine the role of α-hemolysin–mediated activation of NLRP3 in the pathogenesis of *S. aureus* pneumonia. We show that α-hemolysin activates the NLRP3 inflammasome during *S. aureus* pneumonia, inducing necrotic pulmonary injury. Moreover, *Nlrp3*$^{-/-}$ mice have less-severe pneumonia. Pulmonary injury induced by isolated α-hemolysin or live *S. aureus* is independent of interleukin-1β signaling, implicating NLRP3-induced necrosis in the pathogenesis of severe infection. This work demonstrates the exploitation of host inflammatory signaling by *S. aureus* and suggests the NLRP3 inflammasome as a potential target for pharmacologic interventions in severe *S. aureus* infections.**

Community-acquired methicillin-resistant *Staphylococcus aureus* (CA-MRSA) is now the primary cause of skin infections requiring emergency medical attention in the United States [1]. In addition, CA-MRSA can also cause severe, life-threatening infections including necrotizing pneumonias and fasciitis, which are associated with high mortality rates, even in previously healthy patients [2, 3]. These necrotizing infections are among the most severe complications of *S. aureus* infection and are characterized by localized necrosis and inflammation.

All *S. aureus* produce secreted exotoxin virulence factors, including several cytolysins: α-hemolysin, β-hemolysin, and bicomponent leukocidins [4]. α-Hemolysin is one of several critical virulence factors in a murine model of *S. aureus* necrotizing pneumonia, including those caused by CA-MRSA [5, 6]. Purified α-hemolysin induces pulmonary inflammation in rats and rabbits [7–9]. Immunization with inactive α-hemolysin or pharmacologic inhibition of α-hemolysin can prevent or reduce the severity of *S. aureus* pneumonia in mice [10–12]. The mechanisms by which α-hemolysin increases the virulence of *S. aureus* in necrotizing pneumonia are not fully understood.

The nucleotide-binding domain and leucine-rich repeat containing gene family, pyrin domain containing 3 protein (NLRP3) inflammasome is a signaling complex that activates procaspase-1, the processing and secretion of the cytokines interleukin (IL) 1β and IL-18, and the

Received 16 August 2011; accepted 14 October 2011; electronically published 25 January 2012.

Presented in part: 2010 International Conference on Gram-positive Pathogens, Omaha, Nebraska, 10–13 October 2010 (oral presentation); 2010 Keystone Symposium: Innate Immunity: Mechanisms Linking with Adaptive Immunity, Dublin, Ireland, 7–13 June 2010 (D3, poster number 179).

[a]Present affiliation: Department of Pathology, Saint Louis University School of Medicine, St Louis, Missouri.

Correspondence: Joseph A. Duncan, MD, PhD, Department of Medicine, Division of Infectious Diseases, University of North Carolina School of Medicine, 130 Mason Farm Rd, Chapel Hill, NC 27599-7030 (jaduncan@med.unc.edu).

The Journal of Infectious Diseases 2012;205:807–17

DOI: 10.1093/infdis/jir846

initiation of programmed cellular necrosis [13–16]. The NLRP3 inflammasome is activated in response to many pathogen-derived molecules, sterile inducers of inflammation, and microbial pore-forming toxins [17–20]. We recently demonstrated that *S. aureus* α-hemolysin induces NLRP3-mediated signaling in cultured cells [21]. *S. aureus* β-hemolysin and γ-hemolysin also activate the NLRP3 inflammasome, suggesting that numerous *S. aureus* virulence factors converge on this common host-signaling pathway [22]. We sought to investigate whether the activation of the NLRP3 inflammasome was important in the pathogenesis of these infections.

METHODS

Ethics Statement

All protocols were conducted in accordance with National Institutes of Health guidelines for the care and use of laboratory animals and approved by the Institutional Animal Care and Use Committee of the University of North Carolina at Chapel Hill.

Bacteria, Mice, and Reagents

S. aureus strain Newman and the α-hemolysin–deficient isogenic strain (Newman *hla::erm*) were provided by Dr Juliane Bubeck Wardenburg (University of Chicago) [5, 6]. Wild-type mice were from Jackson Laboratory (Bar Harbor, Maine). *Nlrp3*$^{-/-}$ and *Il1r1*$^{-/-}$ mice, back-crossed onto the C57BL/6J genetic background for 9 and 6 generations, respectively, were from Dr John Bertin (Millennium Pharmaceuticals) and Dr Jacques Peschon (Immunex; Amgen). *S. aureus* α-hemolysin (Sigma-Aldrich) was previously determined to be ~50% pure and to activate the NLRP3 inflammasome without triggering Toll-like receptor–dependent pro–IL-1β production [21]. The endotoxin content of the α-hemolysin was determined to be <0.003 International Endotoxin Units/μg of toxin using a chromogenic limulus amebocyte lysate (ToxinSensor; Genscript).

Lung Cell Preparation

Lung sections were incubated in 2.5 mg/mL collagenase/0.5 mg/mL DNase-1 (Sigma-Aldrich) at 37°C for 60 minutes. Red blood cells were lysed with ammonium chloride potassium-containing lysing buffer (Gibco). Single-cell suspensions were adjusted to 2×10^6/mL in complete medium and then stimulated with heat-killed *S. aureus* (HKSA; 1 particle/cell; Invivogen), 10 μg/mL *S. aureus* α-hemolysin (Sigma-Aldrich), or both for 4 hours. CD11b$^+$ cells were purified using anti-CD11b magnetic microbeads according to the protocol provided by the manufacturer (Miltenyi Biotec).

Lactate Dehydrogenase Release, Cytokines, and High-Mobility Group Box 1 Measurements

Lactate dehydrogenase release, enzyme-linked immunosorbent assay (ELISA) for IL-1β and tumor necrosis factor (TNF) α, and high-mobility group box 1 (HMGB1) immunoblot analyses were carried out as described by Craven et al [21]. HMGB1 levels were analyzed using the HMGB1 ELISA kit (IBL International). IL-6 and macrophage inflammatory protein 1α levels were determined using BioPlex multiplex cytokine analysis (BioRad).

Murine Pneumonia and Pneumonitis

Inoculi were prepared from *S. aureus* grown for 5 hours at 37°C in tryptic soy broth after 1:100 dilution of an overnight culture. The bacteria were washed and suspended in phosphate-buffered saline (PBS) at a concentration of 2×10^9 colony-forming units/mL, confirmed by colony counting of plated dilutions of the suspension. Age-matched (10–13-week-old) and sex-matched mice were anesthetized, hung in an upright position by their incisors, and inoculated with 50 μL of PBS containing *S. aureus*, HKSA, or α-hemolysin into the buccal cavity; the nares were blocked to induce aspiration. Intrarectal temperature of infected mice was monitored with a Thermalert TH-5 (Physitemp). Arterial oxygen saturation and pulse distention were determined using the MouseOx pulsoximeter (STARR Life Sciences) in nonanesthetized mice. For studies of lung mechanics, infected mice were given vancomycin (3 mg/d) intraperitoneally starting 4 hours after inoculation.

Bronchoalveolar Lavage Collection, Cell Counts, and Bacterial Burden

Mice were euthanized by CO_2 asphyxiation, the trachea was canulated, and the lungs were flushed 3 times with 1 mL of 0.5 mmol/L ethylenediaminetetraacetic acid (EDTA-Dulbecco's PBS; Invitrogen). Total cell counts were determined using a Neubauer hemacytometer. Polymorphonuclear cell counts were determined by microscopic analysis of cells prepared using the CytoSpin 4 cytocentrifuge (Thermoscientific) and visualized using Quik-Dip Stain (Mercedes Medical). Bronchoalveolar lavage fluid (BALF) and aseptically excised lungs, spleens, and kidneys were collected from euthanized animals. Organ homogenates were prepared in sterile Whirl-Pack bags (Nasco), and serial dilutions were plated in duplicate on mannitol salt agar plates (BD). Bacterial burdens were determined by colony counting after overnight incubation.

Lung Mechanics Studies

Mice were anesthetized and then paralyzed with sequential intraperitoneal injection of 70–90 mg/kg pentobarbital sodium (American Pharmaceutical Partners) and 0.8 mg/kg pancuronium bromide (Baxter Healthcare). Invasive measurements of lung mechanics, including dynamic resistance and dynamic and static compliance, were performed using a computer-controlled small animal ventilator (flexiVent system; Scireq), as described elsewhere [23].

Histology

Mouse lungs were inflated with 10% buffered formalin (20-cm pressure), processed, stained with hematoxylin-eosin

stain, and analyzed microscopically. The extent of lung pathology was scored as described in Supplemental Table 1. The total pathologic score for each mouse was calculated as the sum of scores from each category for that individual. All hematoxylin-eosin–stained sections were scored by a veterinary pathologist (Jackson Laboratory), who was blinded to treatment conditions.

Statistical Analysis

Statistical analysis was performed using GraphPad software by Prism. All data are expressed as means ± standard error of the mean. In experiments in which only 2 groups were studied, an unpaired Student *t* test was used to determine significance. Significance in differences between multiple groups was analyzed by analysis of variance with Bonferroni as a posttest. Survival curves were created using the Kaplan–Meier method and compared using the log-rank (Mantel-Cox) test. In all cases, differences were considered statistically significant at $P < .05$.

RESULTS

α-Hemolysin Activation of NLRP3 Inflammasome in Pulmonary Macrophages

We have reported that human acute monocytic leukemia cell line, THP1 cells, and murine peritoneal macrophages process and secrete IL-1β in response to treatment with HKSA and purified recombinant α-hemolysin. In these studies, HKSA induced pro–IL-1β production, whereas α-hemolysin triggered NLRP3-dependent caspase-1 activation and pro–IL-1β processing [21]. Because α-hemolysin is a critical virulence factor in murine pneumonia models, we sought to determine whether it could induce NLRP3 signaling in cells from mouse lungs. Mixed lung cell preparations treated with α-hemolysin secreted modest levels of IL-1β, regardless of whether they were pretreated with HKSA (Figure 1*A*). To examine the response of pulmonary macrophages to α-hemolysin treatment, CD11b+ cells were isolated from these mixed preparations. These cells secreted higher levels of IL-1β after treatment with either α-hemolysin or HKSA followed by α-hemolysin than preparations depleted of CD11b+ cells (Figure 1*B*). α-Hemolysin did not induce IL-1β secretion in mixed or CD11b+ cells from *Nlrp3*$^{-/-}$ mice (Figure 1*A* and 1*B*). α-hemolysin–induced IL-1β secretion did not require prestimulation (Figure 1*B*). Supernatants from lung cell preparations induced pro–IL-1β expression when applied to THP1 cells (Figure 1*C*), suggesting that pro–IL-1β is up-regulated in the lung cells as a result of the preparation method rather than constitutive high-level expression.

We also sought to determine whether NLRP3-mediated signaling was activated by α-hemolysin in vivo. HKSA, α-hemolysin, and HKSA+α-hemolysin were administered to mice by intratracheal instillation. Six hours after instillation of HKSA (5×10^8 particles, a lethal dose of living *S. aureus*), BALF contained minimal IL-1β and robust levels of TNF-α (Figure 1*D* and 1*E*). Treatment with α-hemolysin alone did not induce TNF-α or IL-1β secretion. Instillation of HKSA+α-hemolysin induced detectable IL-1β, which was markedly diminished in the *Nlrp3*$^{-/-}$ mice (Figure 1*D*). Because instillation of both HKSA and α-hemolysin was required for pulmonary IL-1β production, it is likely that a priming step that induces pro–IL1β production is required for α-hemolysin–induced IL-1β secretion in vivo, as has been documented in cell culture systems [21]. The addition of HKSA+α-hemolysin induced less TNF-α in BALF from wild-type mice compared with HKSA treatment alone, and BALF TNF-α followed a similar trend in *Nlrp3*$^{-/-}$ mice (Figure 1*E*). Thus, HKSA-induced TNF-α secretion may be carried out by cells that do not express NLRP3, or α-hemolysin may interfere with signaling pathways for TNF-α production independent of NLRP3.

NLRP3 Mediation of α-Hemolysin–Induced Pulmonary Injury

We also characterized the pulmonary pathology associated with HKSA+α-hemolysin treatment. Despite the difference in IL-1β secretion between wild-type and *Nlrp3*$^{-/-}$ mice treated with HKSA+α-hemolysin at 6 hours, no animals survived >12 hours (data not shown). To further investigate α-hemolysin–induced pulmonary pathology, mice were given a sublethal dose of HKSA+α-hemolysin (HKSA, 5×10^7 particles; α-hemolysin, 0.5 μg). After 24 hours, the BALF of HKSA+α-hemolysin–treated animals demonstrated robust neutrophilia, which was markedly diminished in the *Nlrp3*$^{-/-}$ animals (Figure 2*A*). *Nlrp3*$^{-/-}$ mice also exhibited less lung pathology in a composite histopathologic index (Figure 2*B* and 2*C*) and individual indices of alveolar and vasculitic inflammation (data not shown). Thus, NLRP3 activation plays an important role in α-hemolysin–induced pulmonary injury and inflammation.

Intratracheal HKSA+α-hemolysin induced severe hypothermia and labored respiration, a syndrome similar to pneumonia induced by living bacteria. The clinical consequences of intratracheal HKSA (1×10^8 particles), α-hemolysin (1 μg), or HKSA+α-hemolysin were studied in wild-type mice. Although mice completely recovered from treatment with HKSA alone, treatment with α-hemolysin resulted in ∼40% mortality and treatment with HKSA+α-hemolysin induced 80%–100% mortality (Figure 2*D* and 2*E*). *Nlrp3*$^{-/-}$ mice were protected from death when compared with their wild-type counterparts (Figure 2*E*). Surviving *Nlrp3*$^{-/-}$ mice were less hypothermic and recovered more rapidly than wild-type mice (Figure 2*F*). These data suggest that NLRP3-induced inflammation plays a significant role in the clinical phenotype of α-hemolysin–induced pneumonitis.

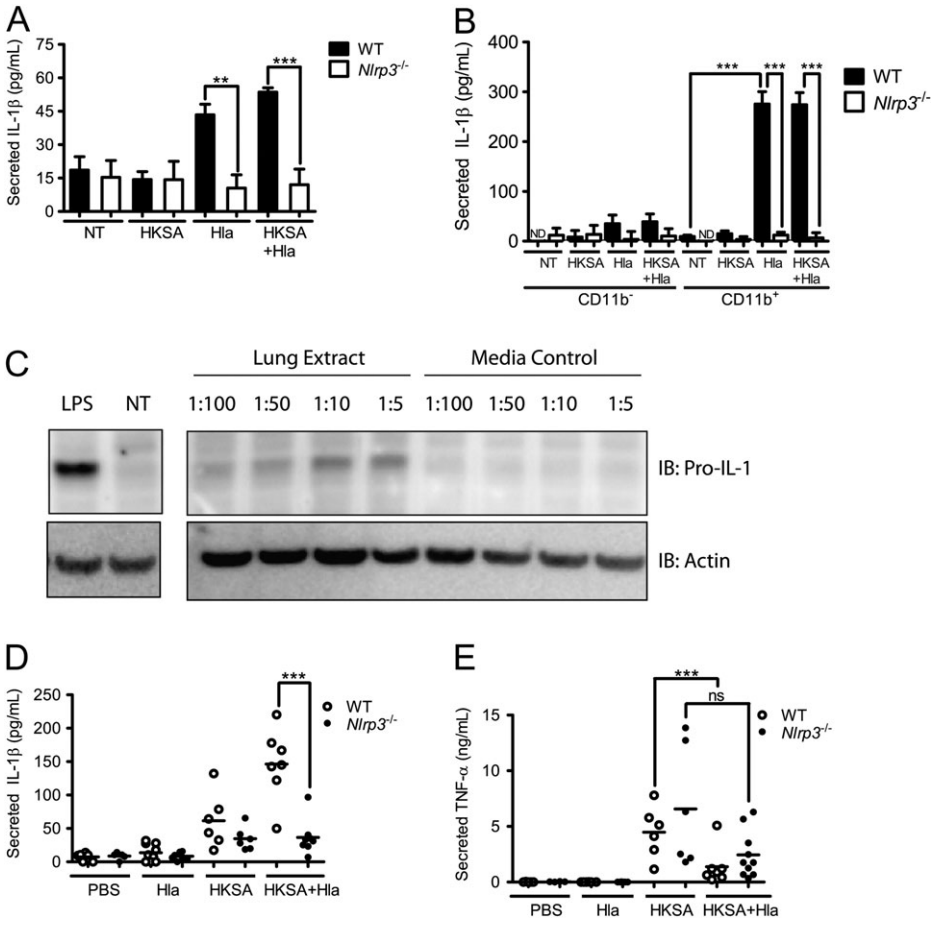

Figure 1. *Staphylococcus aureus* α-hemolysin induces nucleotide-binding domain and leucine-rich repeat containing gene family, pyrin domain containing 3 protein (NLRP3) inflammasome–mediated interleukin (IL) 1β secretion in pulmonary macrophages and murine lungs. *A*, Cells were isolated from the lungs of wild-type (WT) and *Nlrp3*$^{-/-}$ C57L/B6 mice and left untreated (NT) or treated with heat-killed *S. aureus* (HKSA), alpha-hemolysin (Hla), or a combination of the two. Secreted IL-1β was measured in the culture supernatant using enzyme-linked immunosorbent assay (ELISA). *B*, Mouse lung cells were prepared and separated into CD11b^{+} and CD11b^{-} populations using paramagnetic particle-based separation. The cells were treated as described for *A*, and IL-1β secretion was assessed by ELISA. *C*, THP-1 cells were treated with the indicated dilutions of lung cell preparation supernatant or untreated preparation medium as a negative control for 4 hours. Cells were also treated with lipopolysaccharide (LPS) (1 μg/mL; 4 hours). Cell pellets were analyzed by immunoblot with antibodies against pro–IL-1β (3ZD (*upper panel*) and actin (*lower panel*). The samples and controls are from the same immunoblot; however, these samples were not in adjacent lanes. A representative immunoblot from duplicate experiments is shown. *D, E*, C57BL/6 WT and *Nlrp3*$^{-/-}$ mice were anesthetized and phosphate-buffered saline (PBS), HKSA (5×10^8), Hla (1 μg), or a combination of HKSA and Hla was instilled intratracheally. *D, E*, Bronchoalveolar lavage fluid was collected at 6 hours and analyzed for IL-1β (*D*) and tumor necrosis factor (TNF) α (*E*) by ELISA. Bars represent mean ± standard error of the mean of 3 experiments. Statistical significance was determined by 1-way analysis of variance with Bonferroni test. $^{**}P = .001-.01$; $^{***}P < .001$. Abbreviation: ns, not significant.

Effect of α-Hemolysin–Mediated Activation of NLRP3 on Severity of *S. aureus* Pneumonia

Because IL-1β is important in host clearance of *S. aureus* from skin infection models, we used a murine model to further delineate the role of NLRP3 inflammasome activation in *S. aureus* pneumonia. Wild-type mice experienced severe hypothermia and markedly diminished pulse distention consistent with severe systemic inflammatory response within 24 hours of *S. aureus* administration. *Nlrp3*$^{-/-}$ mice were less hypothermic and had increased pulse distention compared with their wild-type counterparts (Figure 3*A* and 3*B*). In mice surviving to 48 hours, *Nlrp3*$^{-/-}$ animals were less hypoxemic than wild-type mice (Figure 3*C*). The overall mortality in this model of *S. aureus* pneumonia was lower in *Nlrp3*$^{-/-}$ mice (14% mortality) than in wild-type mice (37% mortality), but this difference was not statistically significant (data not shown). Compared with wild-type mice, *Nlrp3*$^{-/-}$ mice exhibited significantly better survival free of severe pneumonia, as defined by death, oxygen saturation <95%, or a temperature drop >10°C (Figure 3*D*).

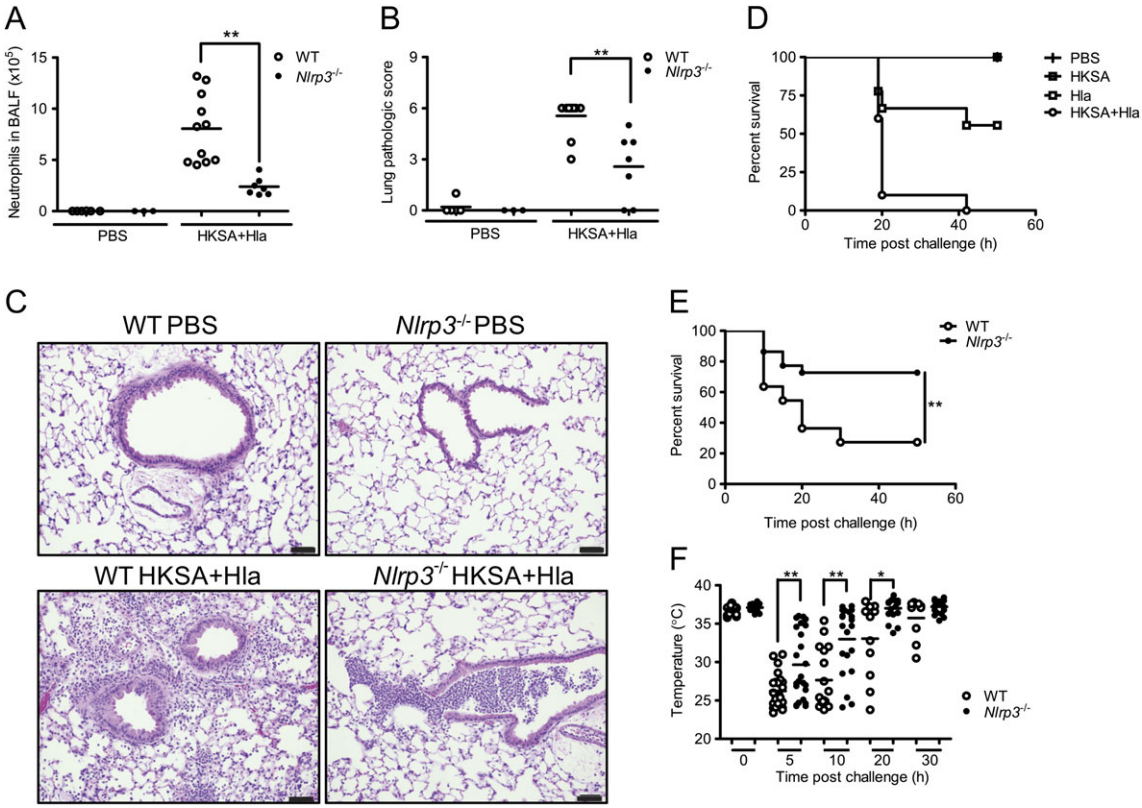

Figure 2. α-Hemolysin induces nucleotide-binding domain and leucine-rich repeat containing gene family, pyrin domain containing 3 protein (NLRP3)–dependent acute pulmonary inflammation and injury. *A–C*, C57BL/6 wild-type (WT) and *Nlrp3*$^{-/-}$ mice were challenged intratracheally with 5×10^7 heat-killed *Staphylococcus aureus* (HKSA) and 0.5 μg Hla (HKSA+Hla) or phosphate-buffered saline (PBS). Bronchoalveolar lavage fluid (BALF) was collected at 24 hours and the lungs were subsequently inflated, fixed, and stained with hematoxylin-eosin (HE). *A,* BALF collected at 24 hours was processed for neutrophil counts. *B,* HE-stained lung sections were stained and scored on a pathologic index that includes alveolar neutrophilic inflammation, vasculitis and vascular extravasation, and bronchial epithelial sloughing or necrosis, as described in the Methods section. *C,* Representative photomicrographs of HE-stained lung tissue from WT and *Nlrp3*$^{-/-}$ mice, harvested 24 hours after challenge with PBS or 5×10^7 HKSA and 0.5 μg Hla (HKSA+Hla). Scale bar, 50 μm. *D,* C57BL/6 WT mice were anesthetized and treated with intratracheal PBS, HKSA (10^8), Hla (1 μg), or a combination of HKSA and Hla. Survival was monitored over a 60-hour time course, as detailed in the Methods section, and is shown by Kaplan–Meier plot. *E, F,* WT and *Nlrp3*$^{-/-}$ C57BL/6 mice were treated with a combination of intratracheal α-hemolysin (1 μg) and HKSA (10^8), as described for *D*. *E,* Survival and intrarectal temperature of survivors was monitored for 60 hours. Survival of mice from each group is shown by Kaplan–Meier plot. Statistical significance was determined by log-rank test, $P < .05$. *F,* Intrarectal temperature is plotted for all surviving animals at each time point. Values are expressed as means ± standard error of the mean. Statistical significance was determined by 1-way analysis of variance with Bonferroni test. $^{**}P = .001-.01$; $^{***}P < .001$.

The consequences of severe *S. aureus* pneumonia on lung function were determined in surviving mice. Wild-type and *Nlrp3*$^{-/-}$ mice were treated with vancomycin, an antibiotic used to treat severe *S. aureus* infections, at the first signs of illness after inoculation with *S. aureus*. All mice survived and normalized their temperature within 3 days (data not shown), and pulmonary function was assessed on day 4. Postpneumonia mice had reduced dynamic lung compliance and increased airway resistance compared with uninfected mice (Figure 3*E* and 3*F*). Along with milder clinical disease, lung compliance was not reduced in *Nlrp3*$^{-/-}$ mice after pneumonia. Thus, the NLRP3 inflammasome plays a key role in mediating pulmonary injury during *S. aureus* pneumonia.

NLRP3 Inflammasome–Induced Inflammation and Clearance of *S. aureus* Pneumonia

Given the unexpected findings that the NLRP3 inflammasome was not protective in murine *S. aureus* pneumonia and that the disease process was worse in *Nlrp3*$^{+/+}$ mice, further studies of the effects of NLRP3 on the host and bacteria during *S. aureus* pneumonia were carried out. Quantitative culture of BALF and lung homogenates revealed that wild-type and *Nlrp3*$^{-/-}$ mice had equivalent *S. aureus* burdens after 24 hours and had almost completely cleared the bacteria by 48 hours (Figure 4*A* and 4*B*). *S. aureus* burdens in the kidneys were low, with no significant difference between wild-type and *Nlrp3*$^{-/-}$ mice with *S. aureus* pneumonia (Figure 4*C*). No dissemination to the spleen was observed in either mouse strain (data not shown). Thus, NLRP3

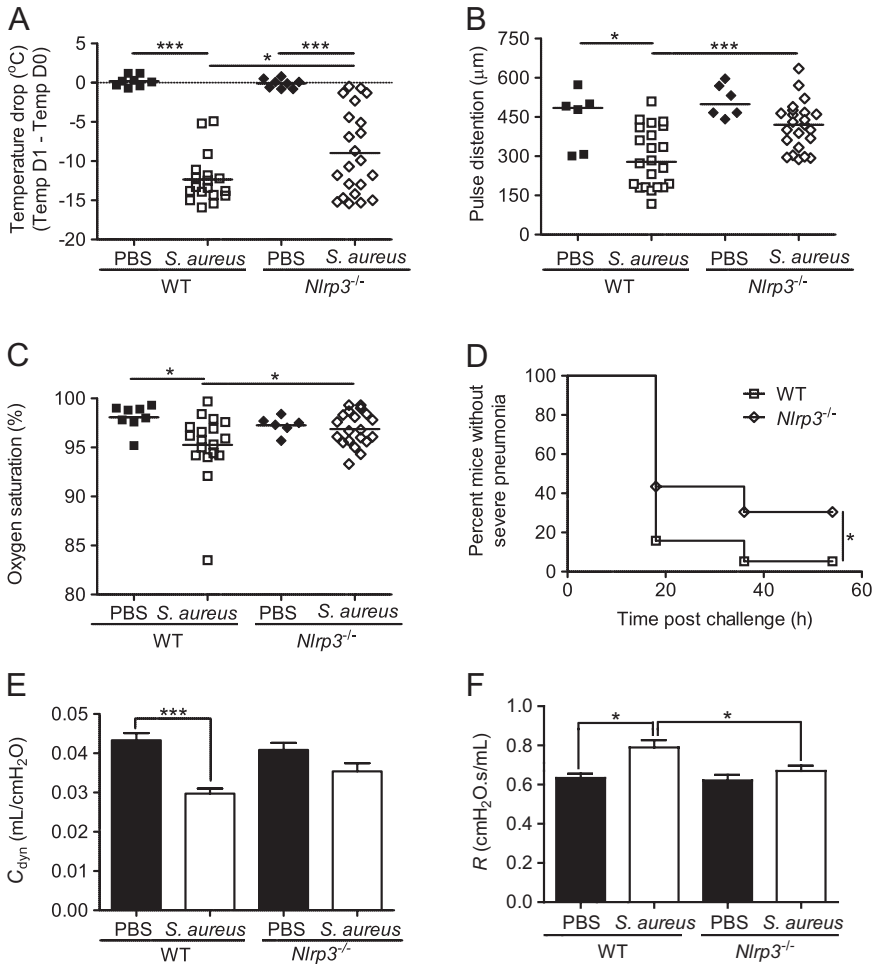

Figure 3. α-Hemolysin–mediated activation of nucleotide-binding domain and leucine-rich repeat containing gene family, pyrin domain containing 3 protein (NLRP3) controls severity of *Staphylococcus aureus* pneumonia. *A–D,* Wild-type (WT) and *Nlrp3*$^{-/-}$ C57BL/6 mice were challenged intratracheally with phosphate-buffered saline (PBS) or 1–2 × 10^8 colony-forming units of live *S. aureus* (strain Newman). *A,* Intrarectal temperature was monitored daily; the change in temperature between day 0 and day 1 (Temp D1 − Temp D0) is plotted for each mouse. Pulse distention and blood oxygen saturation were measured in the mice using a MouseOx small animal pulsoximeter, as described in the Methods section. *B,* Pulse distention 1 day after challenge is plotted for each surviving animal. *C,* Blood oxygen saturation on day 2 is plotted for each surviving animal. Values are expressed as means of 3 independent experiments (n = 6–22 mice per group). Statistical significance was evaluated by 1-way analysis of variance (ANOVA) with Bonferroni test (*$P < .05$, ***$P < .001$). *D,* Composite end point defined by death, oxygen saturation <95%, or temperature drop >10°C was used to define severe pneumonia. Survival free of severe pneumonia is shown using the Kaplan–Meier plot. Statistical significance was determined by log-rank test (*$P < .05$). WT and *Nlrp3*$^{-/-}$ C57BL/6 mice were challenged intratracheally with PBS or live *S. aureus* (as above) and subsequently treated with vancomycin. *E, F,* Dynamic compliance (C_{dyn}) (*E*) and pulmonary resistance (*R*) (*F*) were measured and control mice were compared with pneumonia survivors (all mice survived with vancomycin administration); n = 4–8 mice per group. Statistical significance was evaluated by 1-way ANOVA with Bonferroni test. *$P < .05$; ***$P < .001$.

inflammasome activity does not influence clearance of *S. aureus* during pulmonary infection.

We also examined the role of NLRP3 in the inflammatory response to live *S. aureus* pneumonia. As expected, *Nlrp3*$^{-/-}$ mice had reduced levels of IL-1β in BALF and lung homogenates (Figure 4*D* and 4*E*). TNF-α (Figure 4*F*), IL-6 (not shown), and macrophage 300 inflammatory protein 1α (not shown) levels in BALF were similar between wild-type and Nlrp32/2 mice. Thus, *Nlrp3*$^{-/-}$ mice had reduced IL-1β levels during *S. aureus* pneumonia, while production of other inflammatory cytokines and chemokines was largely intact.

Wild-type mice with *S. aureus* pneumonia had hemorrhagic lungs on gross examination, and the *Nlrp3*$^{-/-}$ mice had pink, healthy-appearing lung tissue (Figure 4*G*). The BALF samples from *Nlrp3*$^{-/-}$ mice with *S. aureus* pneumonia contained fewer neutrophils than their wild-type counterparts (Figure 4*H*). Histologic examination also revealed significantly less pulmonary pathology in the *Nlrp3*$^{-/-}$ mice using a composite index

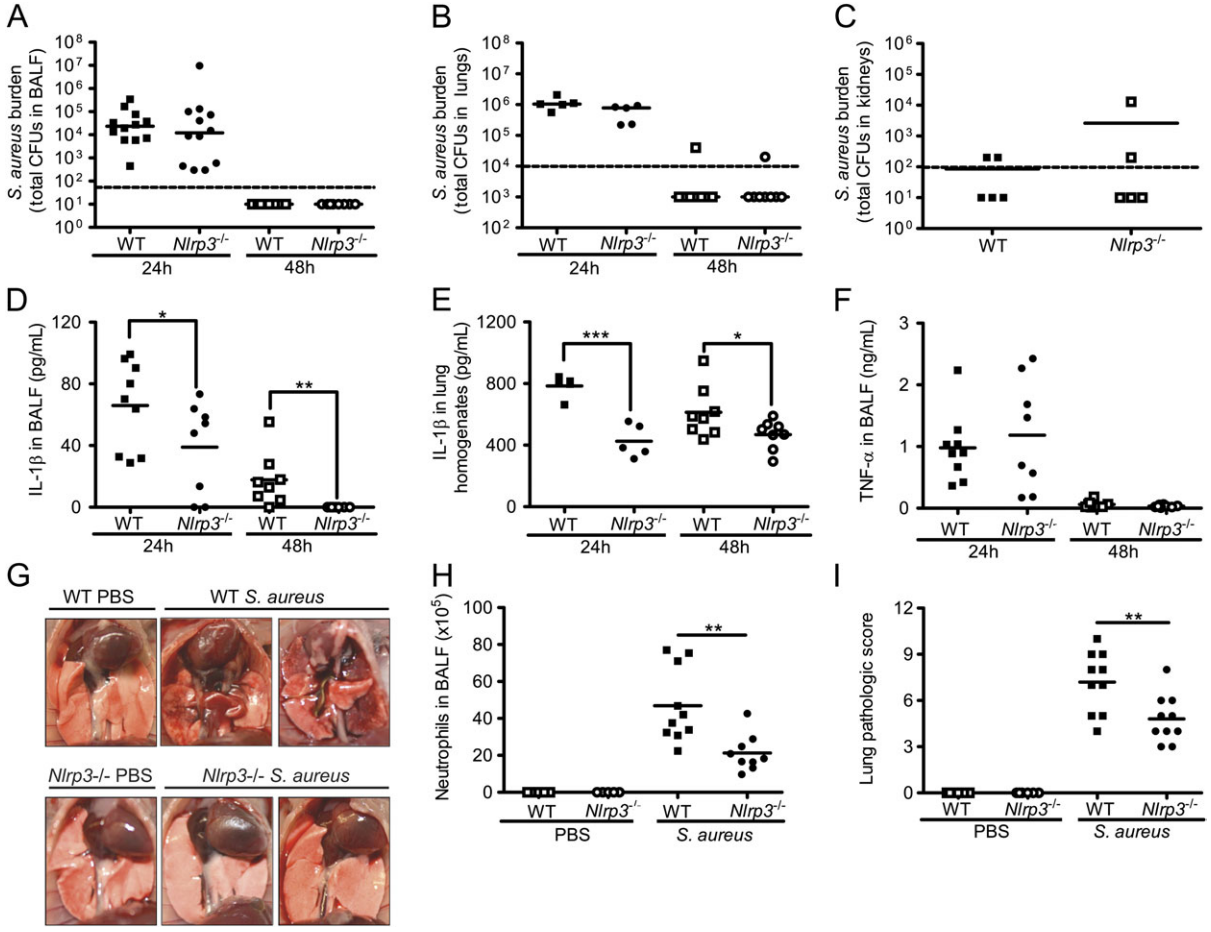

Figure 4. Nucleotide-binding domain and leucine-rich repeat containing gene family, pyrin domain containing 3 protein (NLRP3) inflammasome activation controls inflammation but not bacterial growth during *Staphylococcus aureus* pneumonia. *A–H*, Wild-type (WT) and *Nlrp3*$^{-/-}$ mice were instilled intratracheally with 1–2 × 10^8 colony-forming units (CFU) *S. aureus* (strain Newman). *A–C*, Bronchoalveolar lavage fluid (BALF) samples (*A*), lung homogenates (*B*), and kidney homogenates (*C*) were harvested at 24 and 48 hours then assessed for the presence of bacteria by plating of serial dilutions on mannitol salt agar plates. Dashed lines represent limit of detection (100 total CFU). Statistical significance was determined by 1-way analysis of variance (ANOVA) with Bonferroni test and no significant differences were present (n = 5–12 mice per group). *D–F*, Levels of IL-1β in BALF samples (*D*), interleukin (IL) 1β in lung homogenates (*E*), and tumor necrosis factor (TNF) α in BALF samples (*F*) were determined by enzyme-linked immunosorbent assay. *G*, Lungs from WT and *Nlrp3*$^{-/-}$ C57BL/6 mice infected with live *S. aureus* Newman were exposed and photographed to show gross pathology in situ at day 4. Control mice treated with phosphate-buffered saline (PBS) are shown for comparison. *H*, Total number of neutrophils in BALF samples was determined 24 hours after challenge and represented as means for 5–10 mice per group. *I*, HE-stained lung sections prepared 24 hours after challenge were examined and scored for pathologic findings, as described in Methods. Levels of pulmonary pathology determined using a combined index that includes alveolar inflammation, vascular inflammation, and epithelial sloughing and necrosis are plotted for each animal. Statistical significance was evaluated by 1-way ANOVA with Bonferroni test. *$P < .5$; **$P = .001–.01$; ***$P < .001$.

(Figure 4*I*). In total, our data suggest that activation of the NLRP3 inflammasome during pneumonia leads to excessive inflammation that is deleterious, rather than protective, to the host lung tissue.

NLRP3 Inflammasome Activation and *S. aureus* Pneumonia Pathogenesis in the Absence of α-Hemolysin

To determine whether α-hemolysin from live *S. aureus* was driving the NLRP3-induced lung pathology, we used an isogenic strain of *S. aureus* with a deletion of the *hla* gene. As reported elsewhere, the *hla*-deficient *S. aureus* was less virulent than α-hemolysin-expressing *S. aureus* (data not shown) [6]. To observe a clinical phenotype, we induced *S. aureus* pneumonia with *hla::erm S. aureus* with a larger dose than was used with wild-type *S. aureus*. There was no difference between wild-type and *Nlrp3*$^{-/-}$ mice in the recovered bacteria in BALF or lung homogenates after challenge with *hla*-deficient *S. aureus* (Figure 5*A* and 5*B*). In contrast to findings with wild-type *S. aureus*, the mouse strains challenged with *hla::erm S. aureus* were equally hypothermic, with no difference in BALF neutrophil

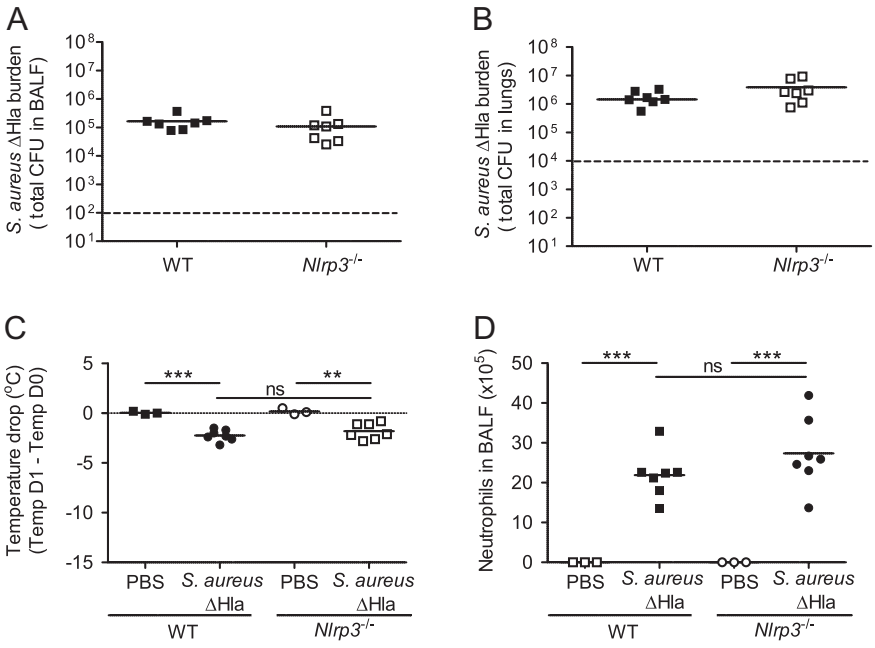

Figure 5. There is no difference in pneumonia severity between wild-type (WT) and *Nlrp3*$^{-/-}$ mice infected with α-hemolysin–deficient *Staphylococcus aureus*. WT and *Nlrp3*$^{-/-}$ animals were intratracheally challenged with 5×10^8 colony-forming units (CFU) of *S. aureus* strain Newman *hla::erm* (a transposon insertion Hla mutant), as described in Methods. *A, B,* Bacterial burden in bronchoalveolar lavage fluid (BALF) samples (*A*) and lung homogenates (*B*) was determined 24 hours after challenge by plating serial dilutions on mannitol salt agar. *C,* Intrarectal temperature was monitored daily; the change in temperature from day 0 to day 1 (Temp D1 − Temp D0) is plotted for each animal. PBS, phosphate-buffered saline. *D,* Total number of neutrophils was measured in BALF samples collected 24 hours after challenge. Statistical significance was determined by 1-way analysis of variance with Bonferroni test (bars represent means. $^{**}P = .001-.01$, $^{***}P < .001$. Abbreviation: ns, not significant.

counts (Figure 5*C* and 5*D*). These data support the hypothesis that activation of NLRP3 is a major mechanism by which α-hemolysin mediates induction of severe *S. aureus* pneumonia.

Role of IL-1β in α-Hemolysin Induced Pulmonary Injury and Promotion of *S. aureus* Virulence

Anti-IL-1 therapy is highly efficacious in the treatment of periodic fever syndromes in patients with mutations in the *Nlrp3* gene, suggesting that processing and secretion of IL-1β is the primary downstream signaling event of NLRP3 inflammasome activation [24–26]. We sought to determine whether excessive IL-1β signaling induced by α-hemolysin was involved in *S. aureus* virulence. First, we studied the effects of intratracheal HKSA+α-hemolysin intoxication in *Il1r1*$^{-/-}$ mice. Unlike *Nlrp3*$^{-/-}$ mice, HKSA+α-hemolysin–treated *Il1r1*$^{-/-}$ mice had mortality and hypothermia equivalent to that in wild-type mice (Figure 6*A* and 6*B*). We also studied pneumonia with live *S. aureus* in wild-type and *Il1r1*$^{-/-}$ mice. Survival free from severe pneumonia (Figure 6*C*) and absolute mortality (not shown) was also indistinguishable between strains. *Il1r1*$^{-/-}$ mice with *S. aureus* pneumonia also had worse blood oxygen saturation than wild-type mice (Figure 6*D*). Combined, these data suggest that the pathogenic mechanism of α-hemolysin–mediated NLRP3 activation during *S. aureus* pneumonia does not require production of IL-1β.

Because α-hemolysin enhanced *S. aureus* virulence through a mechanism that was NLRP3 dependent and IL-1 signaling independent, we sought to examine additional NLRP3-dependent signaling pathways in CD11b+ cells and in mice. Similar to our findings with IL-1β secretion, α-hemolysin induced NLRP3-dependent death that was accompanied by release of HMGB1, a marker of programmed necrosis in CD11b+ cells (Figure 6*E*—*G*). Cell death was not significantly induced in the CD11b-negative cells by this concentration of α-hemolysin (data not shown). HMGB1 levels were also increased in BALF from HKSA+α-hemolysin–treated wild-type mice but not *Nlrp3*$^{-/-}$ mice, confirming that NLRP3 mediates α-hemolysin–induced necrotic cell death in vivo (Figure 6*H*). α-Hemolysin also induced IL-18 secretion from wild-type but not *Nlrp3*$^{-/-}$ CD11b+ cells (Figure 6*I*). IL-18 levels were increased in BALF from wild-type mice with *S. aureus* pneumonia but not *Nlrp3*$^{-/-}$ mice (Figure 6*J*).

DISCUSSION

S. aureus produces many virulence factors, including both surface proteins and exotoxins that have been shown to be

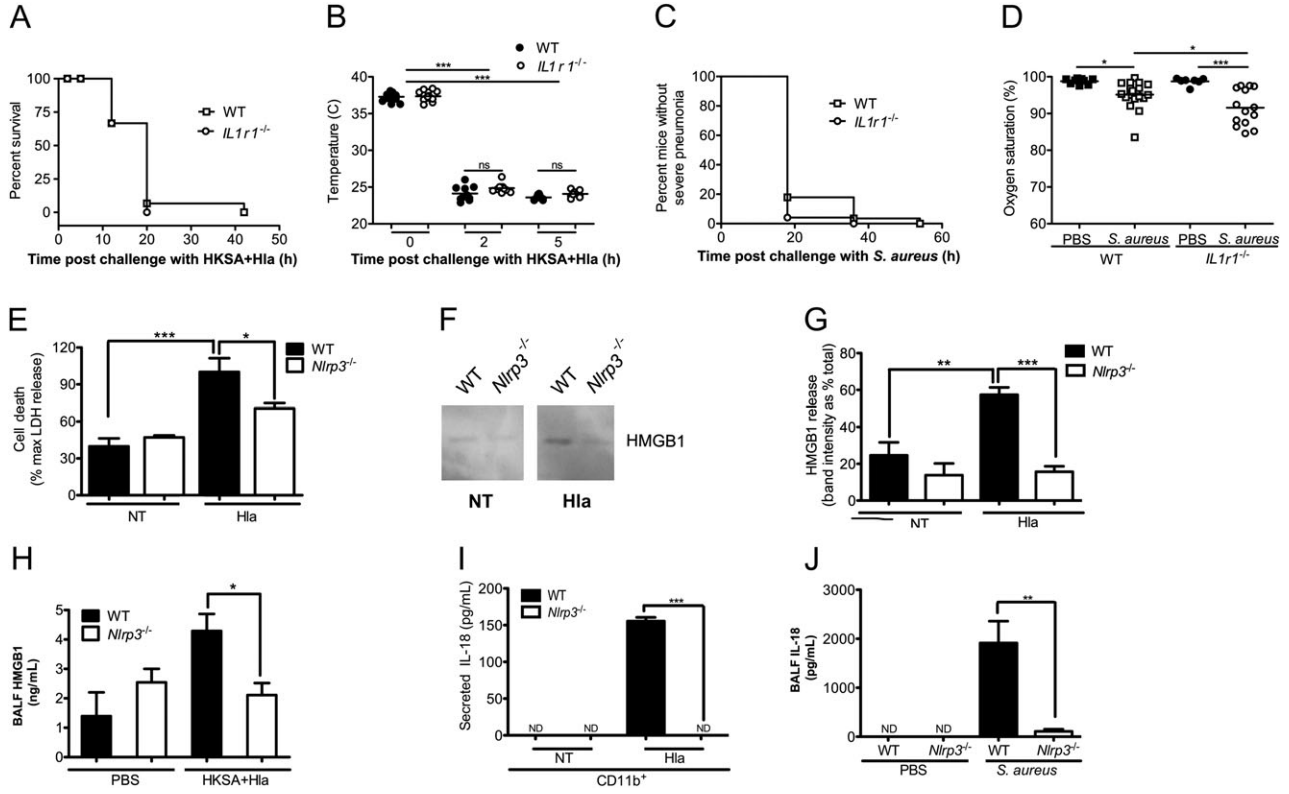

Figure 6. Interleukin (IL) 1β secretion is not responsible for lung injury induced by α-hemolysin–mediated activation of nucleotide-binding domain and leucine-rich repeat containing gene family, pyrin domain containing 3 protein (NLRP3). *A, B*, C57BL/6 wild-type (WT) and *Il1r1*$^{-/-}$ mice were challenged intratracheally with 1 × 10^8 heat-killed *Staphylococcus aureus* (HKSA) and 1 μg of Hla (HKSA+Hla) or phosphate-buffered saline (PBS), as described for Figure 2. *A,* Survival and intrarectal temperature of survivors was monitored for 60 hours. Survival of mice from each group is shown by Kaplan–Meier plot. *B,* Statistical significance was determined by log-rank test ($P < .05$). Intrarectal temperature is plotted for all surviving animals at each time point. *C, D*, WT and *Il1r1*$^{-/-}$ C57BL/6 mice were challenged intratracheally with PBS or 1–2 × 10^8 colony-forming units (CFU) of live *S. aureus* (strain Newman) and monitored as described for Figure 3. *C*, A composite end point defined by death, oxygen saturation <95%, or temperature drop >10°C was used to define severe pneumonia. Survival free of severe pneumonia is shown by Kaplan–Meier plot. No statistically significant difference was observed between WT and *Il1r1*$^{-/-}$ mice, determined by log-rank test. *D*, Blood oxygen saturation on day 2 is plotted for each surviving animal. Values are expressed as means of 3 independent experiments (n = 6–22 mice per group). CD11b$^+$ pulmonary cells were isolated from WT C57BL/6 and *Nlrp3*$^{-/-}$ mice, as described for Figure 1. CD11b$^+$ cells were prepared and left untreated (NT) or stimulated with α-hemolysin. *E*, Cell death was assessed by measurement of the release of cytoplasmic lactate dehydrogenase (LDH) into the culture medium of CD11b$^+$ cells and is plotted as a percentage of maximum (max) release achieved by treatment with detergent. *F, G*, Necrotic cell death, defined by release of high-mobility group box 1 (HMGB1), was assessed using immunoblot analysis of the cell culture supernatants. *F,* Representative immunoblot showing media from untreated cells (NT) and from α-hemolysin–treated (Hla) CD11b$^+$ cells. *G*, Quantities of HMGB1 were determined using the FluorChemE imaging system and analysis software (Cell Biosystems); the level of HMGB1 in the culture supernatant expressed as a percentage of the total is plotted. *H*, C57BL/6 WT and *Nlrp3*$^{-/-}$ mice were challenged intratracheally with 5 × 10^7 HKSA and 0.5 μg of Hla (HKSA+Hla) or PBS. Bronchoalveolar lavage fluid (BALF) was collected at 24 hours, as described for Figure 2. The levels of HMGB1 (a marker of necrotic cell death) in BALF samples were assessed by enzyme-linked immunosorbent assay (ELISA). *I*, IL-18 secretion was measured using ELISA. *J*, WT and *Nlrp3*$^{-/-}$ mice were challenged intratracheally with PBS or 1–2 × 10^8 CFU of live *S. aureus* and IL-18 secretion in BALF was determined after 24 hours. Bars represent mean ± standard error of the mean of 3 (*E, F, J*) or 4 (*G, H, I*) experiments. Statistical significance was evaluated by 1-way analysis of variance with Bonferroni test. **P* < .5; ***P* = .001−.01; ****P* < .001.

important in murine pneumonia models. Recent studies have focused on the role of α-hemolysin in this model [5]. Numerous host cell types are susceptible to this cytolytic toxin. Although lysis of red blood cells to provide heme as an iron source may play a role in α-hemolysin–mediated virulence in humans, this is not the case in mice, because murine hemoglobin is not recognized by the *S. aureus* hemoglobin receptor [27]. Cytolysis of host epithelial cells and leukocytes must be the primary mechanism by which this toxin mediates virulence in the murine pneumonia. Several studies indicated that the NLRP3 inflammasome may be an important target pathway for α-hemolysin; however, in vivo evidence was lacking [21, 22]. In this study we show that pulmonary macrophages are a target of α-hemolysin activity among cells isolated from murine lungs. *S. aureus* α-hemolysin activates the NLRP3 inflammasome both in cultured cells in

vitro and in the lungs in vivo. Interestingly, α-hemolysin's activity toward other cell types in the respiratory system may be mediated through signaling systems independent of NLRP3, such as a disintegrin and metalloprotease 10 (ADAM10), which is a cellular receptor for α-hemolysin and was recently shown to play an important role in murine *S. aureus* pneumonia [28, 29]. Mice lacking NLRP3 are not completely protected from α-hemolysin-expressing *S. aureus*, suggesting that α-hemolysin promotes virulence through NLRP3-dependent and NLRP3-independent mechanisms.

Given previous reports showing that α-hemolysin activates NLRP3, it was not unanticipated that IL-1β secretion is diminished in *Nlrp3*$^{-/-}$ mice after intratracheal α-hemolysin administration or *S. aureus* pneumonia. However, because IL-1β and other inflammasome components are important in the clearance of *S. aureus* in skin infection models, it is surprising that *Nlrp3*$^{-/-}$ mice are not more susceptible to *S. aureus* pneumonia [30]. *S. aureus* lacking O-acetylated peptidoglycan induces increased inflammasome activation and has decreased virulence in a skin infection model compared with *S. aureus* with O-acetylated peptidoglycan [31]. However, O-acetylation of peptidoglycan also protects the bacteria from lysozyme, making it unclear whether the mechanism leading to the diminished virulence is related to increased inflammasome activation. We report that *S. aureus* pneumonia is slightly more severe in *Il1r1*$^{-/-}$ mice, paralleling previous reports that IL-1β signaling is involved in clearance of *S. aureus* in other models of infection. Mice lacking NOD2, an NLR protein involved in recognition of muramyl dipeptide, have decreased sensitivity to *S. aureus* pneumonia and increased sensitivity to intraperitoneal and cutaneous *S. aureus* infections [32–34]. NOD2 signaling up-regulates production of pro–IL-1β, antimicrobial peptides, and other host defense mechanisms, leaving the mechanism underlying the site-specific phenotypes of *S. aureus* infection in *Nod2*$^{-/-}$ mice still to be determined [35]. It also remains to be determined whether NLRP3 deficiency will carry a consistent phenotype with varying sites of infection.

Although *S. aureus* pneumonia in mice may differ from human disease, α-hemolysin does activate the NLRP3 inflammasome in both human and murine cells. Thus, inhibition of the NLRP3 inflammasome may someday prove to be useful adjunctive therapy to antibiotics in severe *S. aureus* pneumonia. At this time, specific NLRP3 inflammasome inhibitors are not available; however, glyburide, an antihyperglycemic medication, has been shown to have NLRP3-inhibitory effects [36]. Interestingly, a recent analysis of patient survival during infection with *Burkholderia pseudomallei* demonstrated that diabetics taking glyburide had better survival rates than nondiabetics, hinting that inhibition of the NLRP3 inflammasome may indeed be beneficial in some acute human infections [37]. Because the protection from *S. aureus* pneumonia observed in *Nlrp3*$^{-/-}$ mice was independent of IL-1β signaling, IL-1 antagonists, which are efficacious in ameliorating fever syndromes associated with NLRP3 signaling hyperactivity, are unlikely to be beneficial and may be harmful in the setting of *S. aureus* infection [24].

S. aureus produces multiple pore-forming toxins that are implicated in the pathogenesis of severe infections and are capable of activating the NLRP3 inflammasome [38, 39]. The presence of NLRP3-activating, pore-forming toxins in other respiratory pathogens, like pneumolysin in *Streptococcus pneumoniae*, suggests that the NLRP3-induced inflammation may be an important factor in many bacterial pneumonias [40–42]. The ability to activate programmed necrosis at a distance may protect these bacteria from host phagocytes, and inflammatory damage to the pulmonary architecture may facilitate bacterial penetration of the epithelial barrier [7, 43]. Further studies are needed to clarify the role of toxin-mediated activation of NLRP3 in other bacterial pneumonias.

Supplementary Data

Supplementary materials are available at the *Journal of Infectious Diseases* online (http://www.oxfordjournals.org/our_journals/jid/). Supplementary materials consist of data provided by the author that are published to benefit the reader. The posted materials are not copyedited. The contents of all supplementary data are the sole responsibility of the authors. Questions or messages regarding errors should be addressed to the author.

Notes

Acknowledgments. We thank Jenny P. Y. Ting and P. Fredrick Sparling for their insights into these studies. The Imaging and Biomarker Analysis Core of the Southeastern Regional Center of Excellence for Emerging Infections and Biodefense (SERCEB) carried out multiplex cytokine analysis.

Financial support. Studies were supported by the Burroughs Wellcome Fund: Career Award for Medical Scientists (to J. A. D.) and the National Institutes of Health (grants AI057157 [SERCEB Career Development Award] and AI088255 to J. A. D., AI077437 [Lung Disease Model Core] and HL071802 to S. L. T.; and HL048160 to C.M.D.). P. M. B. is a trainee of the University of North Carolina STD and HIV Training Program (grant T32AI007001).

Potential conflicts of interest. All authors: No reported conflicts.

All authors have submitted the ICMJE Form for Disclosure of Potential Conflicts of Interest. Conflicts that the editors consider relevant to the content of the manuscript have been disclosed.

References

1. Moran GJ, Krishnadasan A, Gorwitz RJ, et al. Methicillin-resistant *S. aureus* infections among patients in the emergency department. N Engl J Med **2006**; 355:666–74.
2. Francis JS, Doherty MC, Lopatin U, et al. Severe community-onset pneumonia in healthy adults caused by methicillin-resistant *Staphylococcus aureus* carrying the Panton-Valentine leukocidin genes. Clin Infect Dis **2005**; 40:100–7.
3. Miller LG, Perdreau-Remington F, Rieg G, et al. Necrotizing fasciitis caused by community-associated methicillin-resistant *Staphylococcus aureus* in Los Angeles. N Engl J Med **2005**; 352:1445–53.

4. Diep BA, Otto M. The role of virulence determinants in community-associated MRSA pathogenesis. Trends Microbiol **2008**; 16:361–9.
5. Bubeck Wardenburg J, Patel RJ, Schneewind O. Surface proteins and exotoxins are required for the pathogenesis of *Staphylococcus aureus* pneumonia. Infect Immun **2007**; 75:1040–4.
6. Bubeck Wardenburg J, Bae T, Otto M, Deleo FR, Schneewind O. Poring over pores: alpha-hemolysin and Panton-Valentine leukocidin in *Staphylococcus aureus* pneumonia. Nat Med **2007**; 13:1405–6.
7. McElroy MC, Harty HR, Hosford GE, Boylan GM, Pittet JF, Foster TJ. Alpha-toxin damages the air-blood barrier of the lung in a rat model of *Staphylococcus aureus*-induced pneumonia. Infect Immun **1999**; 67:5541–4.
8. Seeger W, Birkemeyer RG, Ermert L, Suttorp N, Bhakdi S, Duncker HR. Staphylococcal alpha-toxin-induced vascular leakage in isolated perfused rabbit lungs. Lab Invest **1990**; 63:341–9.
9. Seeger W, Bauer M, Bhakdi S. Staphylococcal alpha-toxin elicits hypertension in isolated rabbit lungs. Evidence for thromboxane formation and the role of extracellular calcium. J Clin Invest **1984**; 74:849–58.
10. Bubeck Wardenburg J, Schneewind O. Vaccine protection against *Staphylococcus aureus* pneumonia. J Exp Med **2008**; 205:287–94.
11. Ragle BE, Bubeck Wardenburg J. Anti-alpha-hemolysin monoclonal antibodies mediate protection against *Staphylococcus aureus* pneumonia. Infect Immun **2009**; 77:2712–18.
12. Ragle BE, Karginov VA, Bubeck Wardenburg J. Prevention and treatment of *Staphylococcus aureus* pneumonia with a beta-cyclodextrin derivative. Antimicrob Agents Chemother **2010**; 54:298–304.
13. Dowds TA, Masumoto J, Zhu L, Inohara N, Nunez G. Cryopyrin-induced interleukin 1beta secretion in monocytic cells: enhanced activity of disease-associated mutants and requirement for ASC. J Biol Chem **2004**; 279:21924–8.
14. Agostini L, Martinon F, Burns K, McDermott MF, Hawkins PN, Tschopp J. NALP3 forms an IL-1beta-processing inflammasome with increased activity in Muckle-Wells autoinflammatory disorder. Immunity **2004**; 20:319–25.
15. Willingham SB, Bergstralh DT, O'Connor W, et al. Microbial pathogen-induced necrotic cell death mediated by the inflammasome components CIAS1/Cryopyrin/NLRP3 and ASC. Cell Host Microbe **2007**; 2:147–59.
16. Saito M, Nishikomori R, Kambe N, et al. Disease-associated CIAS1 mutations induce monocyte death, revealing low-level mosaicism in mutation-negative cryopyrin-associated periodic syndrome patients. Blood **2008**; 111:2132–41.
17. Martinon F, Petrilli V, Mayor A, Tardivel A, Tschopp J. Gout-associated uric acid crystals activate the NALP3 inflammasome. Nature **2006**; 440:237–41.
18. Mariathasan S, Weiss DS, Newton K, et al. Cryopyrin activates the inflammasome in response to toxins and ATP. Nature **2006**; 440:228–32.
19. Kanneganti TD, Ozoren N, Body-Malapel M, et al. Bacterial RNA and small antiviral compounds activate caspase-1 through cryopyrin/Nalp3. Nature **2006**; 440:233–6.
20. Sutterwala FS, Ogura Y, Szczepanik M, et al. Critical role for NALP3/CIAS1/Cryopyrin in innate and adaptive immunity through its regulation of caspase-1. Immunity **2006**; 24:317–27.
21. Craven RR, Gao X, Allen IC, et al. *Staphylococcus aureus* alpha-hemolysin activates the NLRP3-inflammasome in human and mouse monocytic cells. PLoS One **2009**; 4:e7446.
22. Munoz-Planillo R, Franchi L, Miller LS, Nunez G. A critical role for hemolysins and bacterial lipoproteins in *Staphylococcus aureus*-induced activation of the Nlrp3 inflammasome. J Immunol **2009**; 183:3942–8.
23. Lovgren AK, Jania LA, Hartney JM, et al. COX-2-derived prostacyclin protects against bleomycin-induced pulmonary fibrosis. Am J Physiol Lung Cell Mol Physiol **2006**; 291:L144–56.
24. Goldbach-Mansky R, Dailey NJ, Canna SW, et al. Neonatal-onset multisystem inflammatory disease responsive to interleukin-1beta inhibition. N Engl J Med **2006**; 355:581–92.
25. Hoffman HM. Therapy of autoinflammatory syndromes. J Allergy Clin Immunol **2009**; 124:1129–38.
26. Hoffman HM, Throne ML, Amar NJ, et al. Efficacy and safety of rilonacept (interleukin-1 Trap) in patients with cryopyrin-associated periodic syndromes: results from two sequential placebo-controlled studies. Arthritis Rheum **2008**; 58:2443–52.
27. Pishchany G, McCoy AL, Torres VJ, et al. Specificity for human hemoglobin enhances *Staphylococcus aureus* infection. Cell Host Microbe **2010**; 8:544–50.
28. Wilke GA, Bubeck Wardenburg J. Role of a disintegrin and metalloprotease 10 in *Staphylococcus aureus* alpha-hemolysin-mediated cellular injury. Proc Natl Acad Sci U S A **2010**; 107:13473–8.
29. Inoshima I, Inoshima N, Wilke GA, et al. A *Staphylococcus aureus* pore-forming toxin subverts the activity of ADAM10 to cause lethal infection in mice. Nat Med **2011**; 17:1310–1314.
30. Miller LS, Pietras EM, Uricchio LH, et al. Inflammasome-mediated production of IL-1beta is required for neutrophil recruitment against *Staphylococcus aureus* in vivo. J Immunol **2007**; 179:6933–42.
31. Shimada T, Park BG, Wolf AJ, et al. *Staphylococcus aureus* evades lysozyme-based peptidoglycan digestion that links phagocytosis, inflammasome activation, and IL-1beta secretion. Cell Host Microbe **2010**; 7:38–49.
32. Kapetanovic R, Jouvion G, Fitting C, et al. Contribution of NOD2 to lung inflammation during *Staphylococcus aureus*-induced pneumonia. Microbes Infect **2010**; 12:759–67.
33. Hruz P, Zinkernagel AS, Jenikova G, et al. NOD2 contributes to cutaneous defense against *Staphylococcus aureus* through alpha-toxin-dependent innate immune activation. Proc Natl Acad Sci U S A **2009**; 106:12873–8.
34. Deshmukh HS, Hamburger JB, Ahn SH, McCafferty DG, Yang SR, Fowler VG Jr. Critical role of NOD2 in regulating the immune response to *Staphylococcus aureus*. Infect Immun **2009**; 77:1376–82.
35. Ting JP, Duncan JA, Lei Y. How the noninflammasome NLRs function in the innate immune system. Science **2010**; 327:286–90.
36. Lamkanfi M, Mueller JL, Vitari AC, et al. Glyburide inhibits the Cryopyrin/Nalp3 inflammasome. J Cell Biol **2009**; 187:61–70.
37. Koh GC, Maude RR, Schreiber MF, et al. Glyburide is anti-inflammatory and associated with reduced mortality in melioidosis. Clin Infect Dis **2011**; 52:717–25.
38. Graves SF, Kobayashi SD, DeLeo FR. Community-associated methicillin-resistant *Staphylococcus aureus* immune evasion and virulence. J Mol Med **2010**; 88:109–14.
39. Ventura CL, Malachowa N, Hammer CH, et al. Identification of a novel *Staphylococcus aureus* two-component leukotoxin using cell surface proteomics. PLoS One **2010**; 5:e11634.
40. McCoy AJ, Koizumi Y, Toma C, et al. Cytotoxins of the human pathogen *Aeromonas hydrophila* trigger, via the NLRP3 inflammasome, caspase-1 activation in macrophages. Eur J Immunol **2010**; 40: 2797–803.
41. McNeela EA, Burke A, Neill DR, et al. Pneumolysin activates the NLRP3 inflammasome and promotes proinflammatory cytokines independently of TLR4. PLoS Pathog **2010**; 6:e1001191.
42. Toma C, Higa N, Koizumi Y, et al. Pathogenic Vibrio activate NLRP3 inflammasome via cytotoxins and TLR/nucleotide-binding oligomerization domain-mediated NF-kappa B signaling. J Immunol **2010**; 184: 5287–97.
43. Rose F, Dahlem G, Guthmann B, et al. Mediator generation and signaling events in alveolar epithelial cells attacked by *S. aureus* alpha-toxin. Am J Physiol Lung Cell Mol Physiol **2002**; 282:L207–14.